Inorganic Chemistry

ARTICLE

pubs.acs.org/IC

Photochemistry of *trans*-Cr(cyclam)$(ONO)_2^+$, a Nitric Oxide Precursor

Alexis D. Ostrowski,[†,∥,⊥] Ryan O. Absalonson,[†,∥,⊥] Malcolm A. De Leo,[†,∥,⊥] Guang Wu,[†] James G. Pavlovich,[†] Janet Adamson,[‡] Bilal Azhar,[‡] Alexei V. Iretskii,[§] Ian L. Megson,[‡] and Peter C. Ford*[,†]

[†]Department of Chemistry and Biochemistry, University of California, Santa Barbara, Santa Barbara, California 93106-9510, United States

[‡]Free Radical Research Facility, Department of Diabetes and Cardiovascular Science, University of the Highlands & Islands, Inverness, IV2 3JH, Scotland, U.K.

[§]Department of Chemistry & Environmental Sciences, Lake Superior State University, Sault Ste. Marie, Michigan 49783, United States

Supporting Information

ABSTRACT: Experimental and density functional theory (DFT) studies are described that are focused on outlining the reactivity of the known photochemical nitric oxide precursor *trans*-Cr(cyclam)-$(ONO)_2^+$ ("CrONO", cyclam = 1,4,8,11-tetrazacycltetradecane). Studies in both aerated and deaerated aqueous media are described as are the roles of both the oxidant O_2 and a reductant such as glutathione in trapping the apparent Cr(IV) photoreaction intermediate *trans*-Cr(cyclam)$(O)(ONO)^+$. Also reported and characterized structurally is the Cr(V) product of long-term photolysis in the absence of reducing agents, the *trans*-dioxo species [*trans*-Cr-(cyclam)$(O)_2$](ClO_4). Photosensitization experiments indicate that at least a significant fraction of the reaction occurs from the lowest energy doublet excited state(s). Lastly, cell culture experiments demonstrate that CrONO has little or no acute toxicity either before or after photolysis.

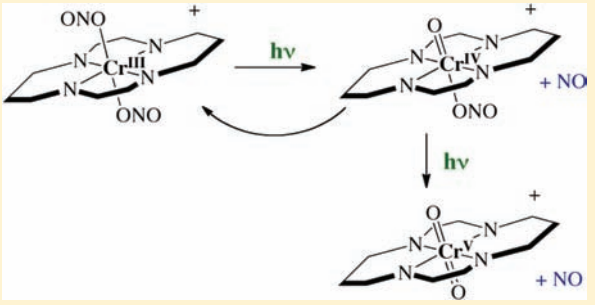

INTRODUCTION

Nitric oxide (also known as nitrogen monoxide) is an endogenous intercellular regulator of numerous physiological processes including vasodilation,[1] some of which are effected at subnanomolar concentrations.[2] NO also plays key roles in cancer biology and has been implicated in both tumor growth and suppression,[3] a dichotomy that is defined by local concentrations, since NO regulation of signaling pathways is both concentration and time-dependent.[4] There is considerable interest in utilizing direct release of cytotoxic NO concentrations in cancer chemotherapy.[5,6] However, the complexity and variability of cellular response to NO suggest that such therapeutic applications of NO donors should be concomitant and synergistic with another cytotoxic therapy.[4a,6a,7] For example, a potentially therapeutic role of NO is as a radiation sensitizer.[7] Malignant tumors have hypoxic regions that are much more radio-resistant than normoxic tissue, and as a consequence, γ-radiation doses necessary to destroy a malignancy exacerbate collateral damage to surrounding healthy tissue. Hypoxia-induced cell resistance may be alleviated by introducing a radiation sensitizer and/or a vasodilator, and targeted NO delivery at a tumor site would serve both functions.

In these contexts, there has been considerable interest in our laboratory[8] and others[9,10] in developing strategies for the release of NO in targeted tissues using excitation with light as the demand signal. A key advantage of photochemical triggering (compared to thermal activation) of appropriate precursors is the precise control that photoexcitation provides regarding the timing, location, and dosage for administration of a bioactive agent. Such control is essential for effective therapy using nitric oxide.

Transition metal nitrosyl complexes have been attractive photochemical NO precursors in many laboratories owing to their sensitivity to excitation at visible wavelengths. A somewhat different precursor is the chromium(III) dinitrito complex ion, *trans*-Cr(cyclam)$(ONO)_2^+$ ("CrONO", cyclam = 1,4,8,11-tetrazacycltetradecane), which we first reported in 1999 to undergo reversible photoinduced cleavage of the CrO−NO bond[11] to give NO plus an intermediate concluded to be a Cr(IV) oxo complex ($Cr^{IV}O$) as illustrated in eq 1.

We have since described the synthesis of CrONO[11b] and of several derivatives with pendant chromophores,[12] and demonstrated that excitation of such chromophores was followed by energy transfer to the Cr^{III} center and sensitized photohemistry.[12,13] We have also further demonstrated

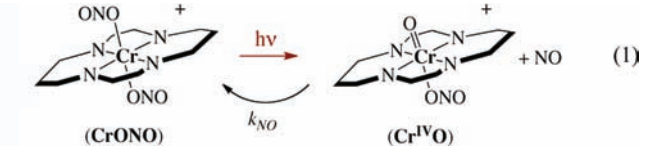

(1)

that the NO released by visible range photolysis activates the key enzyme soluble guanylyl cyclase, both in vitro and in coronary

Received: January 16, 2011
Published: April 08, 2011

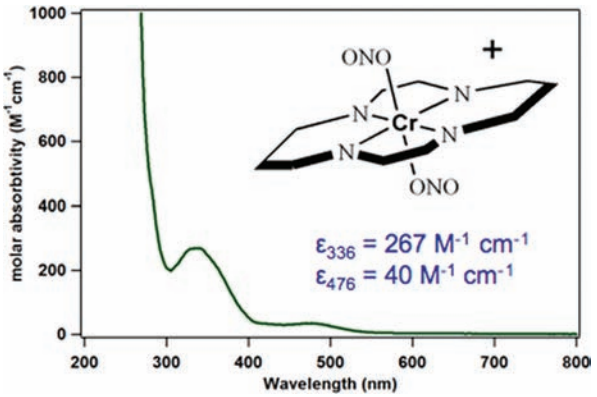

Figure 1. Electronic absorption spectrum of *trans*-[Cr(cyclam)-$(ONO)_2$][BF_4] in aqueous solution.

arterial rings, despite limitations imposed by the very weak visible range, Laporte forbidden d-d absorption bands of this complex (Figure 1).[14] In the present article, we will describe quantitative investigations of this photochemical NO precursor in various aqueous media. We also describe the effect of CrONO and its photoproducts on the viability of cell cultures to probe the question of acute toxicity. Fragments of these studies were reported in the publications noted above, but the goal here is to collate fundamental aspects of those reports with a larger body of unpublished studies to provide a more cohesive picture of the relevant photochemistry.

EXPERIMENTAL SECTION

Synthesis of *trans*-[Cr(cyclam)$(ONO)_2$]BF_4. *Trans*-[Cr-(cyclam)Cl_2]Cl was synthesized according to published procedures.[15] The *trans*-[Cr(cyclam)$(ONO)_2$]BF_4 salt was prepared from the dichloro complex according to a method slightly modified from that of De Leo et al.[11b] Briefly, *trans*-[Cr(cyclam)Cl_2]Cl (50 mg) was dissolved in deionized (DI) water (<5 mL) containing 20 equiv of $NaNO_2$. The purple solution was refluxed in the dark for 2 h, after which the resulting orange solution was cooled slightly and excess $NaBF_4$ was added to give an orange precipitate. The solution was allowed to cool overnight in the refrigerator to complete the precipitation. The orange *trans*-[Cr-(cyclam)$(ONO)_2$]BF_4 (CrONO) was then collected by filtration, and the crude product was recrystallized from methanol to give a material with spectroscopic properties identical to those reported for this well characterized compound.[11b] Yield: 75%. ESI-MS^+: 344 (corresponding to the mass of the *trans*-[Cr(cyclam)$(ONO)_2$]$^+$ cation) with other ions at m/z 314 (CrONO − NO)), 284 (CrONO − 2NO)), and 267 (CrONO −NO, −ONO, −H)). High-resolution mass spectroscopy (FAB-MS^+) was used to resolve the exact formula of the parent ion for CrONO at 344 m/z. HR mass calcd. for M^+ $CrC_{10}H_{24}N_6O_4BF_4$: m/z 344.127426; found 344.126413 (−2.9 ppm)). UV−vis spectrum in water: λ_{max} (ε) 475 nm (40 M^{-1} cm^{-1}), 336 nm (267). Anal. Calcd for $CrC_{10}H_{24}N_6O_4BF_4$: Cr, 12.06. found: Cr, 12.08.

Nitric Oxide Analysis. Two methods were used for the quantitative analysis of NO generated thermally in control reactions or by photolysis of CrONO solutions. The first involved in situ solution electrochemical measurements[16] using an Innovative Instruments inNO-700 nitric oxide specific electrode operating with an Innovative Instruments inNO-T electrostat connected to a computer. The electrode was polarized overnight in salt-water prior to use. At the beginning of each experiment, it was equilibrated in the sample solution for at least 20 min, as determined by a leveling of the response over time. Each experiment recorded current (pA) versus time in the stirred solution. The response was converted from current to [NO] based on a calibration done immediately prior to the experiment. Electrodes were permanently stored in a water bath once put into use. The most common method for generating NO for calibrations was nitrite reduction in acidic iodide solution.

The other NO analysis method utilized a GE Nitric Oxide Analyzer (model NOA-280i). This quantitatively measures the NO entrained from a reaction solution by a flowing gas, typically helium, for measurements under deaerated conditions or medical grade compressed air for aerated conditions. The NOA was calibrated by injection of standard $NaNO_2$ solutions from 5 to 100 μM into a potassium iodide solution in glacial acetic acid. Although both methods are quite sensitive, the NOA generally proved more reproducible owing to inherent instabilities of the electrodes. *Note*: the NOA measurement requires continually removing the NO from the solution by entraining with a gas while the electrode measurement is of a stirred solution in a closed vessel. *Hence, the two experiments are fundamentally different.*

Mass Spectral Studies. Electrospray mass spectra were recorded in the UCSB Mass Spectrometry Facility with a VG Fisons Platform II single quadrupole mass spectrometer using an electrospray ionization source run with a Fisons MassLynx data system. Sample introduction was accomplished either by direct infusion from a Harvard Apparatus Model 22 syringe pump with a Hamilton 250 μL gastight syringe and a Valco stainless steel syringe adaptor or by flow injection from a Michrom BioResources UMA micro HPLC system flowing at 20−50 μL per minute using pure water as solvent and a 50 μL peak injection loop. The inlet capillary for electrospray injection was 34 gauge stainless tubing.

Photochemical Studies. Solutions for continuous studies were prepared in the dark in pH 7.4 phosphate buffer (15 mM). The CrONO concentration was typically ~400 μM. For measurements under deaerated conditions, solutions were prepared in a Schlenk cuvette.[17] The solutions were deaerated by freeze/pump/thaw methods, where the solution was first frozen by cooling to liquid nitrogen temperature, the flask was evacuated and then backfilled with argon after which the solution was thawed and allowed to equilibrate to room temperature. This procedure was repeated 3 times to ensure a deoxygenated medium. Photolysis was then carried out on an optical train equipped with a high-pressure mercury arc lamp excitation source and a mercury line interference filter to isolate the desired excitation wavelength. The intensity of light was determined using ferrioxalate actinometry (for shorter λ_{ex})[18] and Reinecke ion actinometry for longer λ_{ex}.[19] The solution spectra were periodically recorded on a HP8572 diode array UV/vis spectrophotometer to determine the extent of photochemical reaction. Quantum yields were calculated either from the spectral changes or from the amount of NO released.

The NO released upon photolysis of CrONO in pH 7.4 phosphate buffer solution (~100 - 400 μM) was determined using the NOA. Solutions were irradiated (λ_{irr} = 436 nm) for fixed time periods (~5−20 s) while being stirred and entrained with carrier gas that had been passed through a purge vessel filled with DI water. The carrier gas was then passed into the NOA to determine the amount of NO generated. The actual bubbling site was maintained outside the volume of solution directly in the photolysis beam. These experiments were repeated multiple times to ensure a reproducible determination of the NO released.

In some cases, continuous wave photolysis experiments were monitored by both UV/visible absorption spectroscopy and negative ion electrospray mass spectroscopy. In these experiments, all samples were aerated. The lamp intensity, wavelengths selected, UV/visible spectroscopy, and the methodologies for sample irradiation were the same as described above. The main difference in the monitoring of this experiment was additional use of ESMS in a negative ion mode to monitor ionic species generated. After a sample was photolyzed for a predetermined time interval, the UV/visible spectrum was taken and, prior to

being photolyzed again, a 100 μL aliquot was removed from the irradiated solution and infused into the electrospray mass spectrometer. In this case, the injector cone voltage was lowered to 5 V to quell oxidation that occurred with the more typical cone voltage of 30 V. This procedure was repeated after each period of irradiation until the experiment was finished. Dark solutions were similarly probed to evaluate possible competing thermal reactions.

Electron Paramagnetic Resonance (EPR) Studies. A Bruker EMX EPR spectrometer operating at room temperature was used to record EPR spectra both in the solid state and in solutions. The microwave frequency was X-band in both cases. The standard sample used for calibration was 2,2-diphenyl-1-picrylhydrazyl, which is a stable free radical with a g value of 2.0037. Spectra were simulated using 9.0 POWFIT powder spectrum simulation program.[20]

X-ray Data Collection, Structure Solution, and Refinement. A structure is reported for the photoproduct *trans*-[Cr(cyclam)-$(O)_2$]ClO_4.H_2O. A triclinic crystal of approximate dimensions 0.25 × 0.2 × 0.2 mm was mounted on a glass fiber and transferred to a Bruker CCD platform diffractometer. The SMART program[21] was used to determine the unit cell parameters and data collection (20 s/frame, 0.3 deg. /frame for a sphere of diffraction data). The data were collected at room temperature. The raw frame data were processed using the SAINT program.[22] The empirical absorption correction was applied based on ψ-scan. Subsequent calculations were carried out using the SHELXTL program.[23] Crystallographic details and crystal packing are reported in the Supporting Information, Tables S-1 to S-6 and Figure S-1.

DFT Calculations. All calculations were gas phase geometry optimizations performed at the B3LYP/LACVP* level of theory using Spartan '04 or Jaguar 6.0. The energy for the initial and final complexes were determined using the LACVP+* basis set at both the restricted (RODFT) and unrestricted (UDFT) open shell B3LYP levels.

Cell Toxicity Studies. The toxicity of CrONO was investigated with a lactate dehydrogenase (LDH) assay for cell necrosis.[24] This assay indicates when the plasma membrane of the cell has been breached thus releasing LDH and is an indicator of cell toxicity. The human monocytic tumor cell line, THP-1, was used as a model for these studies.

RESULTS AND DISCUSSION

Dark Stability of *trans*-Cr(cyclam)$(ONO)_2^+$. Qualitatively, it has been observed in this laboratory that the d^3 complex CrONO is stable in dark aerated aqueous solutions. To confirm this observation, a pH 7.4 aerated solution of [*trans*-Cr(cyclam)-$(ONO)_2$]BF_4 was thermostatted at 37 °C in the dark and the UV/vis spectra periodically recorded over a period of several days. Slow changes in the visible spectrum (increased absorbance at 336 nm) were seen, and a half-life >30 h was estimated. The absorption changes were much slower at 25 °C.

Photolysis of CrONO in Anaerobic and Aerated Aqueous Solutions. In a preliminary communication,[11a] we described the 436 nm photolysis of CrONO in a stirred pH 7 deaerated aqueous solutions in closed cells. Minimal changes in the optical spectra were observed, namely, modest shifts in the λ_{max} values of the ligand field bands plus small increases in the absorption at ~300 nm. (Supporting Information, Figure S-2). These changes were interpreted in terms of the simple aquation of one axial ligand (eq 2) as has been reported for the dichloro analogue *trans*-Cr(cyclam)Cl_2^+.[25] Consistent with the behavior of the latter complex, the quantum yield as measured by changes in the optical spectra upon exhaustive photolysis deaerated is small (0.009 ± 0.001). This may be considered the upper limit for the quantum yield of ONO^- photoaquation (Φ_{aq}) given that even a small amount of irreversibility of the primary NO release[11a] would give substantially larger absorbance changes (see below). In this context it should be noted that analogous absorption spectra changes were observed under a NO atmosphere, but the quantum yield was smaller (0.004).

$$trans\text{-}Cr^{III}(cyclam)(ONO)_2^+ \xrightarrow{hv} trans\text{-}Cr^{III}(cyclam)(ONO)(H_2O)^{2+} + NO_2^- \quad (2)$$

The photochemistry of CrONO proved to be dramatically different in solutions equilibrated with air. As reported previously, 436 nm photolysis of a stirred, aerobic CrONO solution in a closed cell led to large changes in the UV/vis spectrum (Supporting Information, Figure S-3). Marked increases in the absorbances over the range 270−410 nm were seen with a new λ_{max} at ~312 nm and an isosbestic point at ~266 nm. Furthermore, the quantum yield determined from the spectral changes (Φ_{spec}) in aerobic solution is dramatically higher (0.27 ± 0.03 for 436 nm excitation) than seen in a closed cell under anaerobic conditions. Given the published flash photolysis studies[11a] that demonstrated that the photolabilization of NO from CrONO is reversible (eq 1), this observation can be interpreted in terms of two steps. The first is the primary photochemical reaction, the homolytic cleavage of the CrO−NO bond to give the Cr(IV) intermediate "$Cr^{IV}O$" (eq 1), while the second step would be O_2 trapping of $Cr^{IV}O$ to give Cr(V) product(s) (e.g., eq 3). The latter products were confirmed by observation of Cr(V) signals in the EPR spectra of the products (see below). In the absence of air (or some other trapping agent, see below), $Cr^{IV}O$ reacts with the NO released to regenerate CrONO (eq 1, $k_{NO} = 3.1 \times 10^6$ M^{-1} s^{-1}),[11a] so the only net photoreaction under an argon or NO atmosphere would be the very modest competing photoaquation pathway (eq 2).

$$trans\text{-}Cr^{IV}(cyclam)(ONO)(O)^+ + O_2 \rightarrow Cr(V) + ??? \quad (3)$$

Analogous experiments were carried out with the irradiation wavelengths 365 and 405 nm as well as at 436 nm under a pure dioxygen atmosphere. The measured quantum yield for λ_{irr} 365 nm was a bit lower (0.18 ± 0.02) perhaps because of product inner filter effects, while Φ_{spec} at λ_{irr} 405 nm (0.28 ± 0.03) was indistinguishable from Φ_{spec} at λ_{irr} 436 nm (0.27 ± 0.03). Furthermore, the latter Φ_{spec} value determined in aerobic solution ([O_2] = 270 μM) was the same as that (0.26 ± 0.02) measured under pure O_2 (1.35 mM), indicating that the oxidative trapping of reactive intermediates is already very efficient at the lower [O_2]. Solutions of CrONO underwent identical spectral changes when irradiated at 546 nm over the course of about 1.5 h. Calculating a Φ_{spec} value could not be done accurately owing to the very low absorbance at this λ_{irr}; however, it was clear that the value was at least as large as the Φ_{spec} determined at shorter wavelengths

A key question is: what is the other product(s) of the aerobic oxidation of $Cr^{IV}O$? If this occurs via a simple one electron transfer to O_2, then the "???" represented in eq 3 would be the superoxide ion O_2^-, and indeed our earlier reports suggested this possibility.[11] If this were the case, there are important connotations relevant to the efficiency of NO generation by this photochemical system and its potential application in a physiological context. The reaction of NO with O_2^- occurs at a near diffusion limited rate to give the peroxynitrite anion $ONOO^-$ (eq 4, k_4 = 7×10^9 M^{-1} s^{-1}),[26] another reactive nitrogen oxide species that has drawn considerable interest for its potential roles in

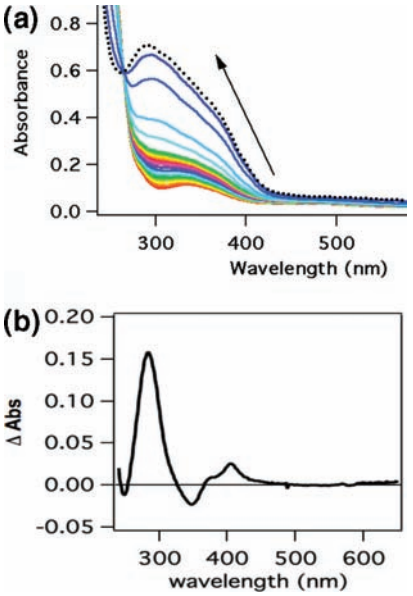

Figure 2. (a) Photolysis of **CrONO** (0.3 mM) (λ_{irr} = 436 nm) in 25 °C in pH 12, aerated aqueous sodium phosphate solution (15 mM). Spectra were taken every 20 s for ~1 h. (b) Difference in the final spectrum after 436 nm photolysis of 0.3 mM CrONO in phosphate buffer at pH 12 vs pH 7.4.

mammalian pathobiology.[27] If peroxynitrite is thus generated, can this pathway be identified and quantified?

$$O_2^- + NO \rightarrow ONOO^- \qquad (4)$$

Once formed in aqueous media, the peroxynitrite ion displays a lifetime that is pH dependent. In acidic solution, it is known to isomerize readily to nitrate ion, but in alkaline solution it is relatively stable and can be identified by its absorption band at 302 nm (ε = 1,670 M^{-1} cm^{-1}).[28] One indication consistent with peroxynitrite formation was seen when CrONO was photolyzed (436 nm) in aerated pH 12 aqueous solution (Figure 2a). Compared to the analogous photolysis of CrONO at pH 7.4 there was a blue shift in the spectrum of the final photoproducts and a significant increase in the absorbance at ~300 nm as seen in the difference spectrum (Figure 2b). That would be expected, if peroxynitrite were generated, given that $ONOO^-$ is stable at pH 12, but not at pH 7.4 where the peroxynitrite ion would be expected to undergo much faster isomerization to the nitrate ion.[29] In contrast, aqueous NO autoxidation leads to nitrite formation,[30] while the low Φ_{aq} photoaquation pathway (eq 2) also releases free nitrite into solution. In this context, the appearance of nitrate as a product of the photolysis would be an indication of peroxynitrite formation as a secondary transient resulting from events starting with the one-electron oxidation of $Cr^{IV}O$.

Mass Spectral Analysis of Photoreaction Products. Evidence supporting the possibility of nitrate formation via the intermediacy of peroxynitrite was probed by negative ion electrospray mass spectrometry of the lighter ions of an aerated aqueous solution of CrONO (100 μM) subjected to 436 nm photolysis. Neither NO_2^- nor NO_3^- was detected in the ESI^- mass spectrum of the solution before initiating the photolysis. However, both NO_2^- (m/z 46) and NO_3^- (m/z 62) were formed in increasing concentrations upon photolysis with a greater fraction of nitrate produced as the experiment proceeded (Figure 3, 10 min intervals for 140 min). The NO_3^-/NO_2^- ratio

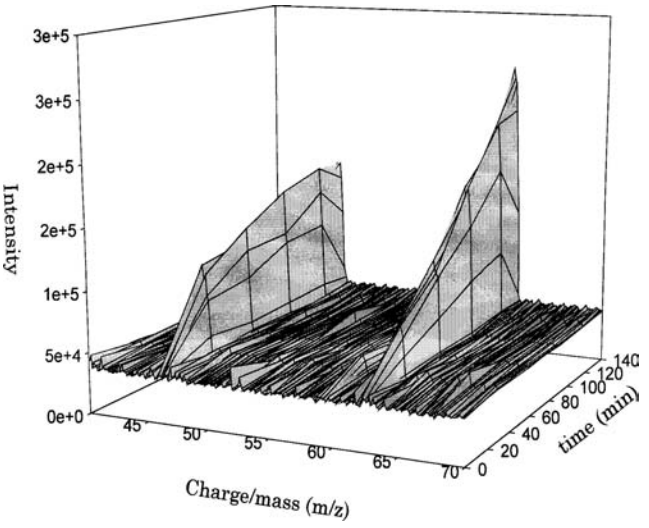

Figure 3. ESI^- MS detection of anions with m/z corresponding to NO_2^- and NO_3^- produced by the 436 nm photolysis of an aerated aqueous solution of CrONO (100 μM). The spectra were recorded for aliquots taken at 10 min intervals for 140 min total irradiation time.

Scheme 1. Illustration of Proposed Redox Reactions Following NO Photodissociation from CrONO

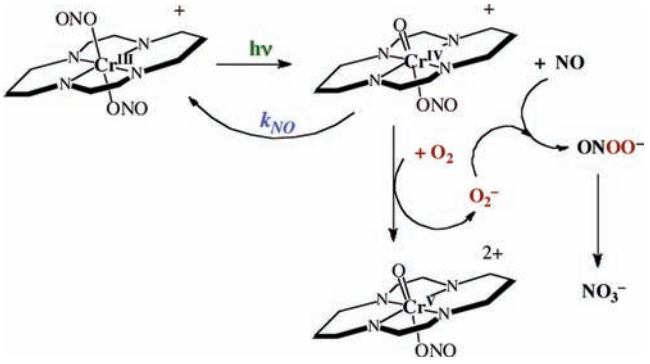

approached 2 to 1 at the later stages (Supporting Information, Figure S-4). As a control, a very dilute solution (0.5 mL) of NO (1.8 μM) was introduced to a closed vial containing air and allowed to react during the course of the photolysis. The ESI^- mass spectrum of this solution, once corrected for background impurities, showed only nitrite ion formation as expected for NO autoxidation in aqueous solution.[30] Thus, we conclude that an intermediate, probably superoxide generated as the result of the oxidative trapping of $Cr^{IV}O$, intercepts at least a fraction of the NO formed by the photoreaction described by eq 1. The proposed sequence of events in an aerobic medium is illustrated by Scheme 1.

Cationic species generated in the photolysis of aerated CrONO solutions were also probed by ESI-MS experiments, this time in the positive ion mode. The situation is more ambiguous given that the complexes themselves undergo some decomposition under the analysis procedure, although setting the cone potential to 5 V minimized the secondary redox reactions that were seen when this was higher (30 V). Aliquots (125 μL) were periodically removed from an aerated pH 7 aq. CrONO solution (300 μM) (298 K) during 436 nm irradiation and analyzed by ES^+ mass

dx.doi.org/10.1021/ic200094x |*Inorg. Chem.* 2011, 50, 4453–4462

Table 1. Positive Ions in Aerated CrONO Photolysis Solution As Analyzed by in ESMS$^+$ and Proposed Assignments

m/z	z	Proposed ionic species
344.0	+1	$(M)^+$ of $[Cr^{III}(cyclam)(OH)(ONO)]^+$
315.0	+1	$(M)^+$ of $[Cr^{III}(cyclam)(OH)(ONO)]^+$ or $(M\text{-}H)^+$ of $Cr^{V}(cyclam)(O)(ONO)]^{2+}$
313.0	+1	$(M\text{-}H)^+$ of $[Cr^{V}(cyclam)(O)(ONO)]^{2+}$
286.0	+1	$(M)^+$ of $[Cr^{III}(cyclam)(OH)_2]^+$
284.0	+1	$(M)^+$ of $[Cr^{V}(cyclam)(O)_2]^+$
266.0	+1	$(M\text{-}2H)^+$ of $[Cr^{V}(cyclam)(O)]^{3+}$
142.5	+2	$(M)^{2+}$ of $[Cr^{V}(cyclam)(O)(OH)]^{2+}$
133.5	+2	$(M\text{-}H)^{2+}$ of *trans*-$[Cr^{V}(cyclam)(O)]^{3+}$

spectrometry. Changes in the spectra were clearly a function of the irradiation time. Before initiating photolysis, the only peak present corresponded to the CrONO ion at *m/z* 344. After 30 min, the intensity of this ion had dropped about 1/3 and new ions appeared at *m/z* 315, 313, 286, 284, 266, 142.5, and 133.5, the last two corresponding to +2 ions. This trend continued over the course of photolysis with a steady growth of the five lighter ions to limiting values as the CrONO ion diminished (see Supporting Information, Figure S-5). The intensities of the cations at *m/z* 315 and 313 began to drop after about 40 min, although these were present throughout the course of the experiment. The peak for CrONO completely disappeared after 140 min of irradiation, but no significant changes took place in the thermal control solution of CrONO during the irradiation time. Possible assignments of these cations consistent with the proposed photolysis pathways are listed in Table 1.

As monitored by ES$^+$ mass spectrometry, the products of exhaustive photolysis (>1000 min) of CrONO were somewhat different when carried out under a dioxygen atmosphere ($[O_2]$ = 1.35 mM) than under a reduced oxygen atmosphere ($[O_2]$ = 0.27 mM). In the former case, the dominant peak corresponded to a 2+ ion at *m/z* 133.5 with substantial peaks corresponding to a 2+ ion at *m/z* 142.5 and a +1 ion at *m/z* 284. In the latter case, the dominant peak (by far) was for the +1 ion at *m/z* 284. These data are consistent with the observations described below regarding the EPR spectra of the solids isolated by adding sodium tetraphenylborate to the solutions formed by exhaustive photolysis of CrONO. The products gave different spectra depending on whether the solution had been equilibrated with pure O_2 or with a much lower O_2 pressure during irradiation.

For the sake of discussion, we propose that in the former case, the principal chromium product is the Cr(V) oxo nitrito complex $Cr^{V}(cyclam)(O)(ONO)^{2+}$, which displays a different fragmentation in the MS than does the dioxo product $Cr^{V}(cyclam)(O)_2{}^+$ formed under low $[O_2]$ conditions. This suggests that under conditions where the O_2 does not efficiently trap the $Cr^{IV}O$ intermediate according to Scheme 1, secondary photolysis of the latter leads to the O_2-independent formation of the Cr(V) dioxo product (eq 5). This proposal is substantiated by the observations that up to 2 NO's per CrONO are generated by exhaustive photolysis under a helium atmosphere, and that $[Cr(cyclam)(O)_2]ClO_4$ can be isolated from such solutions by addition of $NaClO_4$ (see below).

$$trans\text{-}Cr^{IV}(cyclam)(O)(ONO)^+ \xrightarrow{h\nu} trans\text{-}Cr^{V}(cyclam)(O)_2{}^+ + NO \quad (5)$$

Analysis of Photoinduced NO Release. As noted above, the net photochemistry observed by spectral changes upon photolysis of CrONO solutions relies on oxidative trapping of $Cr^{IV}O$. Thus, in a closed system the net NO release will be compromised by the other reactive oxygen species (O_2^- and $ONOO^-$) generated as byproducts of such oxidative trapping. For electrochemical experiments using a nitric oxide specific electrode, it was clear that NO is generated during the photolysis of stirred aerobic CrONO solutions in closed vessels. However, while repeated experiments, gave qualitative reproducibility and indicated a yield much less than that of the Cr(V) products, there was considerable scatter in the quantitative measurements. To address this issue, we turned to the NOA, which analyzes the NO entrained from a reaction medium by a flowing gas. For this experiment, CrONO solutions were photolyzed for specific periods of time while bubbling with medical grade air, and the gas stream was analyzed to quantify the NO. The amount of NO released after each short photolysis is the integrated NO signal following that interval. A sample trace from the NOA involving successive 5 s photolysis periods is shown in Figure 4. The first interval gave a strong signal for NO (0.17 nmoles total), but successive photolysis intervals gave progressively much smaller net NO release.

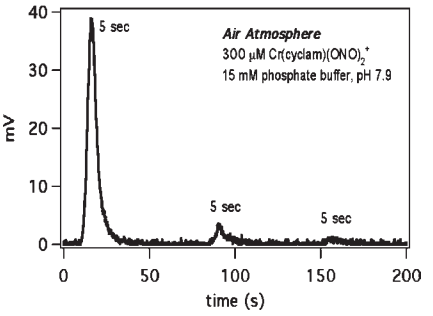

Figure 4. Photoinduced release of NO from an aerated 3 mL volume of CrONO solution (0.3 mM) in pH 7.9 phosphate buffer (15 mM) measured using the NOA (λ_{irr} = 436 nm) The integrated signals correspond to the net NO released during successive 5 s irradiation intervals with the solution being continuously entrained with air.

Given that the initial solution contained 9 μmoles of CrONO, the diminishing yields of NO entrained from the photolysis solution for the NOA experiment illustrated by Figure 4 can not be attributed to rapid depletion of the initial CrONO. Instead, it appears that increasing concentrations of a NO trap (or traps) are accumulating, possibilities being the superoxide proposed above or to some other species, such as peroxynitrite. It should be emphasized that only the NO swept from the solution by the entraining gas would be detected by this technique, and that this process takes ~20 s as indicated by the width of the signals seen. Thus, the magnitude of the signal is a very complex function

dx.doi.org/10.1021/ic200094x |*Inorg. Chem.* 2011, 50, 4453–4462

of the quantity of NO produced by the primary photochemical event (eq 1) and the competition between NO solution-to-entraining-gas transport and NO trapping by solution components. Although, O_2 does react with NO by third order kinetics (second order in [NO]),[30] this reaction cannot be the origin of the behavior seen in Figure 4, since with the flowing air, the dioxygen concentration is constant.

Notably, when the analogous experiment was conducted using the same CrONO concentration, irradiation wavelength and intensity, but with oxygen-free helium as the entraining gas, dramatically larger quantities of NO (1.2 nmoles) were detected by the NOA after the first 5 s irradiation period. Furthermore, subsequent 5 s irradiations of the latter solution showed no decrease in the integrated NO peak intensities (see Supporting Information, Figure S-6). This remarkably different pattern when the sweeping gas is chemically inert clearly points to the role(s) of reactive oxygen species generated under aerobic conditions in scavenging NO. The UV/vis absorption spectrum under flowing He (Supporting Information, Figure S-7) also changes in a manner different from that seen under a static inert atmosphere (Supporting Information, Figure S-2) or in a static aerated solution (Supporting Information, Figure S-3). This reinforces the validity of eq 1 as the primary photoreaction for CrONO and suggests that NO transport into the entraining gas is sufficiently fast to compete effectively with the back reaction of NO with $Cr^{IV}O$. On the other hand, the much greater generation of NO when He rather than air is the entraining gas, even in the first aliquot, indicates that the NO is trapped/scavenged by other species faster in the oxidizing media than it is removed by the entraining gas.

By measuring the release of NO directly using the NOA, the quantum yield of NO production (Φ_{NO}) upon 436 nm photolysis of CrONO in pH 7.4 phosphate buffer solutions (15 mM) was determined to be 0.25 ± 0.03 when the entraining gas was He. Thus the NO release is in good agreement with the Φ_{spec} determined previously from absorbance changes under aerated conditions where $Cr^{IV}O$ is apparently trapped efficiently. This agreement confirms the stoichiometry of the primary photochemical process and demonstrates that NO transport to the entraining He is faster than the back reaction.

When the NOA was used to monitor the NO release from buffered CrONO solutions while irradiating continuously at 436 nm and entraining with He, it was found that the rate of NO production decreased continually as expected for the depletion of the initial reactant. However, long-term photolyses under He consistently gave more than one NO per chromium complex initially present, and continuous irradiation over several hours gave a NO/Cr stoichiometry of nearly 2. Thus, it appears that NO is generated from the second nitrite ion initially present in CrONO. This could be accomplished by secondary photolysis of the $Cr^{IV}O$ intermediate (eq 5) or by some more complex mechanism involving disproportionation of $Cr^{IV}O$. Regardless, the observation of a NO/Cr ratio >1 has implications with regard to the likely products (see below).

Photochemistry in the Presence of Reductants. Formation of peroxynitrite is a potential problem if the photolysis of CrONO is used to generate NO in aerobic environments, since peroxynitrite is a reactive species that can contribute to oxidative stress.[27] While that in itself might not be such an undesirable effect in tumor tissue, it is notable that solid tumors are often hypoxic. Thus, a key question is whether the Cr(IV) intermediate generated in the initial photochemical step (eq 1) would also be

Scheme 2

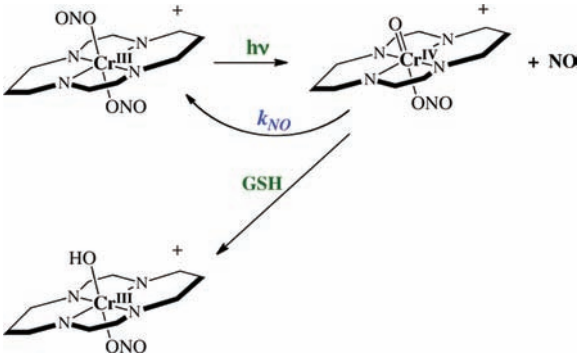

intercepted by biological reductants in processes sufficiently fast to compete with the back reaction. A recent publication from this laboratory[14] demonstrated this to be the case when glutathione (GSH), an important antioxidant in biological tissue,[31] is present in CrONO photolysis solutions. For completeness, we will briefly summarize these studies.

When CrONO was photolyzed (λ_{irr} 436 nm) in pH 7.4 aqueous buffer solution (15 mM phosphate) with added GSH (5 mM), the absorption spectra changes were nearly identical regardless of whether the system was being entrained with air or with He (see Supporting Information, Figure S-8). These observations suggest the formation of the same metal complex product, regardless of the atmosphere, and the product spectra were interpreted in terms of the formation of the Cr(III) complex *trans*-Cr(cyclam)(ONO)(OH)$^+$.[14] Furthermore, the quantum yields of NO release under these respective conditions were measured as 0.19 and 0.25 ± 0.02 using the NOA. Thus, even when dioxygen is present, GSH at these concentrations competes effectively to reduce $Cr^{IV}O$ to a Cr(III) product as indicated in Scheme 2. This is ideal for therapeutic applications where NO needs to be generated in hypoxic, reducing environments that are typical in tumor tissues.[32,33]

An unanswered question regarding Scheme 2 is: What is the other product(s) of the GSH reaction with $Cr^{IV}O$? It is likely that this reaction would generate the glutathione radical GS•, which would either dimerize to the glutathione disulfide (GSSG) or react with NO to give the S-nitrosothiol GSNO (eq 6). However, since S-nitroso thiols are relatively unstable both thermally and photolytically,[34] the observation of nearly quantitative recovery of the NO released is not surprising.

$$NO + GS\bullet \rightarrow GSNO \qquad (6)$$

Further Studies of the Chromium Photoproducts. The above observations suggest that in aerobic media, the chromium photoproducts will be Cr(V) species formed by autoxidation (Scheme 1) or secondary photolysis (eq 5) of the Cr(IV) intermediate(s). The formation of chromium(V) products was confirmed by EPR studies of solids isolated by adding $Na[BPh_4]$ to the solutions formed after exhaustive photolyses of CrONO at high (1.35 mM, sample A) and low (0.27 mM, sample B) O_2 concentrations. Unlike Cr(III) and Cr(IV) species, which are generally EPR silent at ambient temperature, the $3d^1$ Cr(V) species display strong signals.[35] In contrast, solid and solution samples of CrONO gave no EPR signal at room temperature.

dx.doi.org/10.1021/ic200094x |*Inorg. Chem.* 2011, 50, 4453–4462

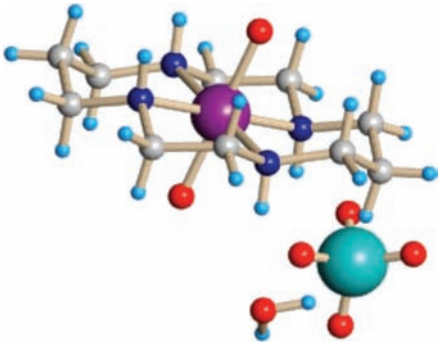

Figure 5. Ball and stick diagram of the square red crystals isolated after addition of $NaClO_4$ to photolyzed aqueous solutions of CrONO. This is isolated as a hydrated perchlorate salt.

The spectrum of solid sample B (Supporting Information, Figure S-9) showed a broad signal consistent with a d^1 species such as *trans*-$Cr^V(cyclam)(O)_2^+$. There appeared to be little or no hyperfine coupling with the equatorial N's of the cyclam ligand. The room temperature EPR spectrum of sample A (Supporting Information, Figure S-10) was more complicated and but could be interpreted in terms of a mixture of Cr(V) species, 60% being the same as that seen in sample B and 40% being another d^1 species, such as *trans*-$Cr^V(cyclam)(O)(ONO)^{2+}$. The latter displays nitrogen hyperfine coupling (A_{xx} = 4.79 and A_{yy} = 22.05) suggesting a spin interaction with a N-containing axial ligand, such as nitrite.

The identity of the *trans*-$Cr^V(cyclam)(O)_2^+$ product was confirmed by isolating the photoproduct from a deaerated pH 7.4 phosphate buffer (15 mM) solution of CrONO (~1 mM) that had been exhaustively photolyzed. A large excess of $NaClO_4$ was dissolved in the solution, and slow evaporation in air yielded large square red crystals. The X-ray crystal structure (Figure 5) indicated this to be [*trans*-$Cr(cyclam)(O)_2]ClO_4 \cdot H_2O$. Detailed structural data are reported in the Supporting Information, Tables S-1 to S-6. Dissolving this material in acetonitrile solution gave a strong, room temperature EPR spectrum (g = 1.99) consistent with that expected for this $3d^1$ Cr(V) complex. A very similar EPR spectrum was reported for the Cr(V) species formed by the spontaneous decomposition of *trans*-$Cr(cyclam)(H_2O)(OOH)^+$.[36]

What Excited States (ES) are Responsible for the Photoreactivity of CrONO? Hexacoordinate Cr(III) complexes have a d^3 electronic configuration with a ground state spin multiplicity of S = 4. In the visible spectrum of CrONO, a spin allowed, Laporte forbidden d-d transition to a quartet excited state, $^4[CrONO] \rightarrow {}^4[CrONO]^*$ is evident at λ_{max} = 476 nm. The lower energy *spin forbidden and Laporte forbidden* d-d transition to the doublet ES $^2[CrONO] \rightarrow {}^2[CrONO]^*$ that is predicted from ligand field theory was not observed, even at high concentrations. This is not surprising, since this band typically has an extinction coefficient $\ll 1\ cm^{-1}\ M^{-1}$. The band at 336 nm was assigned as an intraligand $n \rightarrow \pi^*$ transition of the nitrito ligand,[12,37] but occurs at a wavelength where a second quartet-to-quartet transition is also expected. Observation of facile photodissociation of NO from the *trans*-$Cr(cyclam)(ONO)_2^+$ at longer visible wavelengths, even at λ_{irr} = 546 nm argues that this reactivity occurs from a low energy ligand field (LF) ES, either one of the lowest energy quartet states formed by direct excitation or the even lower energy doublet states formed by intersystem crossing from the quartet state(s).

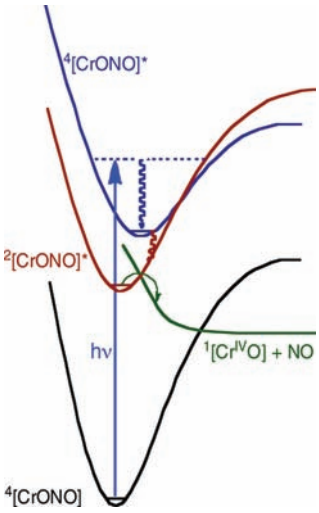

Figure 6. Hypothetical photophysical reaction pathway. Excitation into the quartet excited state followed by intersystem crossing to the reactive doublet excited state from which NO is released.

Figure 6 illustrates a (simplified) possible scenario for the excited state reactivity of CrONO. While the reactive pathway must be from the lowest energy quartet or doublet ES (or both), the doublet pathway is attractive given the apparent spin conservation of NO dissociation: $^2[CrONO]^* \rightarrow {}^1[Cr^{IV}O] + {}^2NO$. If the doublet is the reactive state, it should be possible to achieve the same reactivity by using a photosensitizer to access this state directly. The energy of the doublet state could not be determined directly, since CrONO is not phosphorescent, even at low temperatures. However, the analogous dichloro complex *trans*-[Cr-(cyclam)$(Cl)_2$]Cl shows phosphorescence at 77 K around 700 nm[38] with sharp bands indicative of a 0−0 transition of about 690 nm (~14,490 cm^{-1}). The analogous *trans*-dinitrito complex CrONO would have a very similar doublet 0−0 energy, since ligand field strength has almost little effect on the doublet state energies in d^3 complexes. The energy of the lowest quartet excited state $^4[CrONO]^*$ was estimated by Gaussian analysis of the visible absorption band using the 5% rule[39] (Supporting Information, Figure S-11) to be ~18,340 cm^{-1}, much higher than the doublet excited state $^2[CrONO]^*$. Thus, a photosensitizer with a donor energy between these values should be able to undergo selective energy transfer to the doublet but not to the quartet.

Such a photosensitizer is the organic dye erythrosin B which has an estimated triplet energy of ~16,667 cm^{-1} and a triplet lifetime of 3 ms in aqueous solution.[40] Potential photosensitization was studied by irradiating a deareated pH 7.0 phosphate buffer solution of CrONO (3.1 μM) and erythrosin B with 436 nm light (24.0 °C). The solution was continuously entrained with He, which was subsequently analyzed by the NOA for NO formation. (Notably, the concentrations of dye and NO precursor were very low owing to the sensitivity of the NOA. Higher concentrations of these two components saturated the NOA signal).

Under these conditions the calculated initial absorbances of the solution components were 0.020 for the dye and 0.00011 for chromium substrate. In this context, >99.4% of the incident light that was absorbed was indeed absorbed by the dye. The NOA response reached a maximum of 800 mV with a peak area over a total of 500 s of 44,853, which corresponds to 6.1 nanomoles of NO (Supporting Information, Figure S-12). For comparison, the solution contained 9.3 nmoles of CrONO. When an analogous

dx.doi.org/10.1021/ic200094x |*Inorg. Chem.* 2011, 50, 4453–4462

solution with only CrONO (1.1 μM. 3.3 nmoles in 3 mL) was similarly studied to evaluate the effect of the photosensitizer, it was found that NO was continually formed over a period of 2 h, but the maximum signal was only 25 mV (Supporting Information, Figure S-13). Even taking into account the difference in CrONO concentrations, it is clear that the maximum signal for the sensitized experiment was an order of magnitude larger than for direct excitation of CrONO, strong evidence for erythrosin B acting as a photosensitizer for the generation of NO from CrONO.

It was further noted that the phosphorescence from erythrosin B was substantially (>50%) quenched by concentrations of CrONO comparable to those used in the above photosensitization experiment. However, a Stern−Volmer analysis was not completed upon discovering that the dye apparently degraded during these experiments as evidenced by changes in its absorption and emission spectra, possibly from reaction of erythrosin B or its excited state with the CrONO primary photoproducts NO or $Cr^{IV}O$.

In a similar context, it was noted that increasing concentrations of CrONO, quenched the phosphorescence from the related dicyano complex $Cr(cyclam)(CN)_2^+$ (λ_{max}^{em} = 720 nm, τ = 340 ms).[41] These experiments could be carried out in an aerobic environment, since the emission from the dicyano complex was not affected by air. The k_q rate constant for quenching was relatively small ($\sim 1 \times 10^6$ M^{-1} s^{-1}) as has been noted previously for other nearly isoergic energy transfers between similar Cr(III) complexes.[42] However, it is notable that the ES quenching was accompanied by enhanced photoreactivity from CrONO as evidenced both by changes in the difference spectra and in NO production. Thus, there is little doubt that the doublet excited states are largely responsible for the photogeneration of NO from CrONO both in anoxic and aerated media, although it is difficult to exclude the operation of some prompt photolabilization from the quartet states initially formed upon direct excitation.

DFT Computations. Gas phase geometry optimizations performed at the B3LYP/LACVP* level of theory for CrONO and the primary photolysis products $Cr^{IV}O$ and NO (eq 1). Energies of these species were calculated using the LACVP+* basis set at both the restricted (RODFT) and unrestricted (UDFT) open shell B3LYP levels. The UDFT results all converged and gave energies slightly lower for ground state reactant and product than converged RODFT computations (Supporting Information, Table S-7), so the UDFT results will be used for further discussion. The doublet excited state ^{2}[CrONO]* was calculated to be 0.066 hartree (173 kJ/mol) higher energy than the quartet ground state ^{4}[CrONO]. This corresponds to ~695 nm very close to the doublet energy of the *trans*-dichoro complex (see above). It is notable that the geometry optimization showed the calculated CrO−NO bond to be 0.025 Å longer for ^{2}[CrONO]* (1.386 Å) than for ^{4}[CrONO] (1.362 Å), whereas the CrON−O distance is shorter by 0.008 Å, approaching the calculated value of 1.158 Å for a free NO. (The experimental value of d_{NO} is 1.15 Å). The Cr−O(NO) bond length is correspondingly 0.069 Å shorter (1.878 vs 1.947 Å) for the doublet ES. With regard to the chromium product of the primary photoreaction, these calculations suggest the triplet ^{3}[$Cr^{IV}O$] to be slightly lower energy (0.0042 hartree or 11 kJ/mol) than the singlet ^{1}[$Cr^{IV}O$], in contrast to our expectation.

Energy profiles for the ground and doublet states of CrONO were created by stretching the CrO−NO bond and minimizing the energy of the species so generated (Figure 7 and Supporting Information, Figure S-14). For the ground electronic state, the

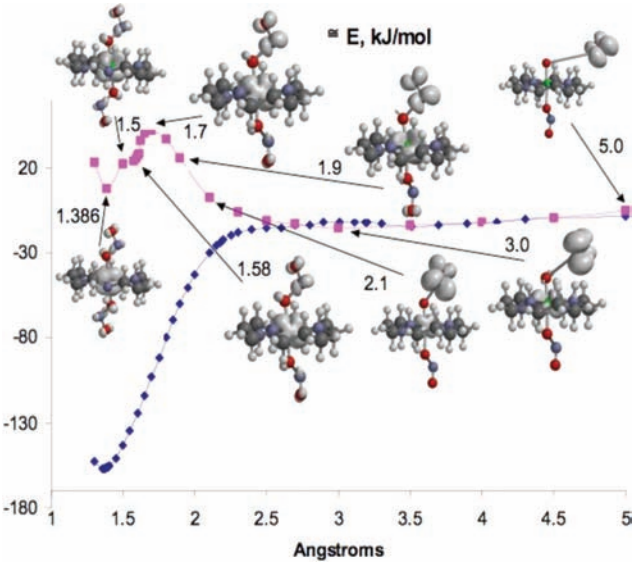

Figure 7. DFT calculated (gas phase) energy profiles (in kJ mol^{-1}) for a process where the CrO−NO bond is stretched toward dissociation starting with the quartet ground state ^{4}[CrONO or the doublet excited state ^{2}[CrONO]*. All energies are referenced to the energy of the products NO plus ^{3}[$Cr^{IV}O$].

energy of the system rises until the bond length is approximately 2.4 Å, then a small dip is observed at 3.5 Å due to van der Waals forces. Correspondingly, the Cr−O(NO) bond length shortens from 1.95 Å to ~1.65 Å as the CrO−NO bond stretches toward dissociation. According to this calculation, there should be very little barrier for the back reaction of $Cr^{IV}O$ with NO, consistent with this reaction indeed having a large second order rate constant,[11a] although, if the barrier were no more than that indicated, one might have expected an even faster second order reaction.

According to the calculated energies listed in Supporting Information, Table S-7, the chemical transformation described by eq 1 is endothermic by 0.0575 hartree (151 kJ/mol) for complete NO dissociation, so the doublet excited state is sufficiently energetic to accomplish this. To evaluate a potential reaction coordinate for NO dissociation, the structural changes, energies, and spin densities were calculated for different CrO−(NO) distances for both the ground electronic state and the doublet excited state (Figure 7). For both it appears that the spin density surfaces surrounding the NO moiety appear to duplicate the π-antibonding molecular orbitals after the CrO−(NO) bond has been stretched beyond 2.4 Å. This implies that NO has fully separated from CrO at any further distance. An interesting feature of this figure is the prediction that NO dissociation from a thermally equilibrated doublet excited state would involve a modest activation energy of approximately 45 kJ/mol. Despite this, quantum yield measurements at 37 °C for NO release using the NOA gave values, within experimental uncertainty, that were the same as those found at 25 °C, However since the doublet is formed by isoergic intersystem crossing from a higher energy quartet state, it is possible that NO dissociation occurs without such thermal equilibration.

Toxicity Studies. To utilize the CrONO complex as a photochemical donor in vivo, the toxicity of CrONO, as well as its photoproduct(s) will need to be evaluated. The toxicity of CrONO was investigated with a lactate dehydrogenase (LDH) assay using the human monocytic tumor cell line, THP-1.

dx.doi.org/10.1021/ic200094x |*Inorg. Chem.* 2011, 50, 4453–4462

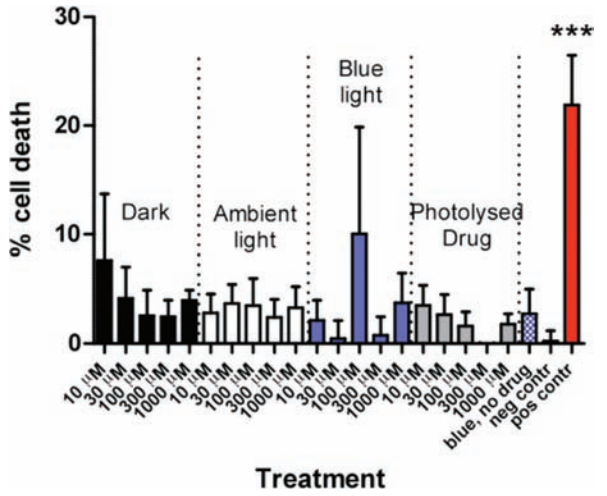

Figure 8. LDH cell viability assay (n = 3) of the viability of human monocytic tumor cells, THP-1 with increasing concentrations of CrONO in the dark (black bars), with ambient light (white bars) and with blue light (470 nm) photolysis (blue). The effect of equivalent concentrations of pre-photolyzed CrONO solutions is indicated by the gray bars, and the effect of blue light alone is shown in blue. The effect of a positive control (H_2O_2; 20 mM) is shown in red. ***$p < 0.001$; one-factor ANOVA with Bonferroni post-test.

The LDH assay is an indicator of cell toxicity, detecting when the plasma membrane of the cell has been breached to release of LDH from the cell. As illustrated in Figure 8, *CrONO did not induce significant toxicity*, even when concentrations of 1000 μM were added to the phenol-red free medium (2 h incubation period). In addition, when CrONO-treated cell cultures were exposed to a blue LED array (ThorLabs) for the entire 2 h treatment period, at a fixed distance of 10 cm from the top of the well (published intensity of the LED at this distance is 600 μW/cm^2 and the wavelength is centered at 470 nm), there was no significant increase in cytotoxicity (the apparent effect at 300 μM CrONO is not statistically different from untreated control). These data indicate that neither the NO photogenerated nor the reactive intermediates proposed above induce *acute* toxicity. Notably, earlier myography experiments[14] using porcine arterial rings showed that irradiation of analogous solutions of CrONO led to vasodilatation with an IC_{50} of 250 nM CrONO. As Figure 8 shows, neither prephotolyzed CrONO solutions nor the blue light alone induced any cytotoxicity, while 20 mM H_2O_2 (positive control) was the only treatment to induce significant LDH release.

Pilot experiments with two other cytotoxicity assays (3-(4,5-dimethylthiazol-2-yl)-2,5-diphenyltetrazolium bromide; MTT for mitochondrial activity and DiOC6 as a marker of mitochondrial membrane potential, a recognized early marker of apoptosis) also failed to show any significant cytotoxic effect of any of the concentrations tested ($\leq$1000 μM), thus confirming that neither CrONO nor the products formed from its photolysis displays acute toxicity under the conditions tested. The relative lack of toxicity even during photolysis of CrONO indicates furthermore that the NO released is not sufficient to trigger NO-mediated cell death. Notably, the rate of photoinduced NO release is relatively low owing to the small extinction coefficient of CrONO at the 470 nm excitation wavelength and corresponding low light absorption. Nevertheless, our previous data confirmed that, under identical photolysis conditions, considerably lower concentrations of CrONO ($\sim$3 μM) were sufficient to induce NO-mediated maximal vasodilation.[14] The result is therefore in keeping with the paradigm that much higher concentrations of NO (μM) are needed to induce cell death than to effect vasodilation (nM).

The above result also provides evidence that, even in oxygenated media, the reducing moieties present, such as GSH, ascorbate, cysteine, and antioxidant enzymes (superoxide dismutase), are sufficient to ensure that toxic levels of reactive oxygen species such as superoxide or peroxynitrite are not formed from CrONO photolysis under these conditions. Peroxynitrite, if generated as suggested above from reaction of superoxide and NO, should lead to substantial cell toxicity.[43] In this context, we can conclude that the reducing moieties must intercept initially formed oxidants such as $Cr^{IV}O$.

SUMMARY

This article has summarized the comprehensive photochemistry of the nitric oxide precursor *trans*-Cr(cyclam)$(ONO)_2^+$ in aerated and deaerated media. CrONO demonstrates several key properties that make it attractive as a photochemical NO precursor in potential therapeutic applications including good thermal stability and substantial quantum yields for the NO release throughout the visible wavelength region. Neither CrONO itself nor its photoproducts show acute toxicity in cell culture experiments despite the formation of several high valent chromium photoproducts in aerobic media, perhaps because these species are intercepted by antioxidants such as glutathione. However, it is also clear that the low extinction coefficients for this compound at longer visible wavelengths will inhibit its effectiveness during in vivo applications. To address this issue, ongoing studies are directed toward preparing CrONO conjugates, with single or two photon absorbing chromophores that can serve as antenna to sensitize the photochemistry of NO release at the longer wavelengths where tissue transmission is optimal.

ASSOCIATED CONTENT

Supporting Information. (A) Data for crystal structure of *trans*-[Cr(cyclam)$(O)_2$]$ClO_4 \cdot H_2O$ (5 tables and figure showing packing diagram. (B) Data concerned with photochemical Studies: 14 Figures showing, variously, changes in absorption spectra, mass spectra of reaction and product solutions, EPR spectra of solid products isolated by precipitation, nitric oxide analyzer data, and results of DFT calculations. This material is available free of charge via the Internet at http://pubs.acs.org.

AUTHOR INFORMATION

Corresponding Author

*E-mail: ford@chem.ucsb.edu.

Notes

[⊥]Taken in part from the Ph.D. dissertations of (a) Ostrowski, A. D. University of California, Santa Barbara, 2010. (b) Absalonson, R. O. University of California, Santa Barbara, 2009. (c) De Leo, M. A. University of California, Santa Barbara, 1998.

Author Contributions

[‖]These authors contributed equally to the experimental studies.

■ ACKNOWLEDGMENT

This work was supported by a NSF grant to P.C.F. (NSF-CHE-0749524). A.D.O. acknowledges the ConvEne IGERT program for a fellowship (NSF-DGE 0801627). We thank Dr. Chosu Khin of UCSB for help with EPR spectra and M.A.D. acknowledges numerous conversations and helpful advice and information on Cr(V) chemistry from Dr. A. Bakac of the Ames Laboratory.

■ REFERENCES

(1) *Nitric Oxide: Biology and Pathobiology*, 2nd ed.; Ignarro, L. J., Ed.; Elsevier Inc.: Burlington, MA, 2010.

(2) Garthwaite, J. *Mol. Cell. Biochem.* **2010**, *334*, 221–232.

(3) (a) Bonavida, B.; Khineche, S.; Huerta-Yepez, S.; Garban, H. *Drug Resist. Updates* **2006**, *9*, 157–173. (b) Fukumura, D.; Kashiwagi, S.; Jain, R. K. *Nat. Rev. Cancer* **2006**, *6*, 521–534. (c) Jenkins, D. C.; Charles, I. G.; Thomsen, L. L.; Moss, D. W.; Holmes, L. S.; Baylis, S. A.; Rhodes, P.; Westmore, K.; Emson, P. C.; Moncada, S. *Proc. Natl. Acad. Sci. U.S.A.* **1995**, *92*, 4392–4396. (d) Wink, D. A.; Vodovotz, Y.; Laval, J.; Laval, F.; Dewhirst, M. W.; Mitchell, J. B. *Carcinogenesis* **1998**, *19*, 711–721. (e) Xie, K.; Huang, S. *Free Radical Biol. Med.* **2003**, *34*, 969–986.

(4) (a) Ridnour, L. A.; Thomas, D. D.; Switzer, C.; Flores-Santana, W.; Isenberg, J. S.; Ambs, S.; Roberts, D. D.; Wink, D. A. *Nitric Oxide* **2008**, *19*, 73–76. (b) Olson, S. Y.; Garban, H. J. *Nitric Oxide* **2008**, *19*, 170–176.

(5) (a) Hickok, J. R.; Thomas, D. D. *Curr. Pharm. Des.* **2010**, *16*, 381–391. (b) Sonveaux, P.; Jordan, B. F.; Gallez, B.; Feron, O. *Eur. J. Cancer* **2009**, *45*, 1352–1369. (c) Rose, M. J.; Mascharak, P. K. *Cur. Opin. Chem. Biol.* **2008**, *12*, 238–44.

(6) Ostrowski, A. D.; Ford, P. C. *Dalton Trans.* **2009**, 10660–9.

(7) (a) Mitchell, J. B.; Wink, D. A.; DeGraff, W.; Gamson, J.; Keefer, L. K.; Krishna, M. C. *Cancer Res.* **1993**, *53*, 5845–5848. (b) Griffin, R. J.; Makepeace, C. M.; Hur, W.-J.; Song, C. W. *Int. J. Radiat. Oncol.* **1996**, *36*, 377–383. (c) Bourassa, J.; DeGraff, W.; Kudo, S.; Wink, D. A.; Mitchell, J. B.; Ford, P. C. *J. Am. Chem. Soc.* **1997**, *119*, 2853–2860.

(8) (a) Ford, P. C.; Bourassa, J.; Miranda, K. M.; Lee, B.; Lorkovic, I.; Boggs, S.; Kudo, S.; Laverman, L. *Coord. Chem. Rev.* **1998**, *171*, 185–202. (b) Ford, P. C. *Acc. Chem. Res.* **2008**, *41*, 190–200.

(9) (a) Tfouni, E.; Krieger, M.; McGarvey, B. R.; Franco, D. W. *Coord. Chem. Rev.* **2003**, *236*, 57–69. (b) Pavlos, C. M.; Xu, H.; Toscano, J. P. *Curr. Top. Med. Chem.* **2005**, *5*, 635–645. (c) Rose, M. J.; Mascharak, P. K. *Coord. Chem. Rev.* **2008**, *252*, 2093–2114. (d) Schatzschneider, U. *Eur. J. Inorg. Chem.* **2010**, 1451–1467. (e) Sortino, S. *Chem. Soc. Rev.* **2010**, *39*, 2903–2913. (f) Kristian, K. E.; Song, W.; Ellern, A.; Guzei, I. A.; Bakac, A. *Inorg. Chem.* **2010**, *49*, 7182–7187.

(10) (a) Megson, I. L.; Holms, S. A.; Magid, K. S.; Pritchard, R. J.; Flitney, F. W. *Br. J. Pharmacol.* **2000**, *130*, 1575–1580. (b) Madhani, M. P.; Apurba, K.; Miller, T. W.; Eroy-Reveles, A. A.; Hobbs, A. J.; Fukuto, J. M.; Mascharak, P. K. *J. Med. Chem.* **2006**, *49*, 7325–7330. (c) Oliveira, F. d. S. F.; Kleber, Q.; Bonaventura, D.; Bendhack, L. M.; Tedesco, A. C.; Machado, S. de P.; Tfouni, E.; Santana da Silva, R. *J. Inorg. Biochem.* **2007**, *101*, 313–320.

(11) (a) De Leo, M.; Ford, P. C. *J. Am. Chem. Soc.* **1999**, *121*, 1980–1981. (b) De Leo, M. A.; Bu, X.; Bentow, J.; Ford, P. C. *Inorg. Chim. Acta* **2000**, *300−302*, 944–950.

(12) DeRosa, F.; Bu, X.; Ford, P. C. *Inorg. Chem.* **2005**, *44*, 4157–65.

(13) Neuman, D.; Ostrowski, A. D.; Mikhailovsky, A. A.; Absalonson, R. O.; Ford, P. C. *J. Am. Chem. Soc.* **2008**, *130*, 168–75.

(14) Ostrowski, A. D.; Deakin, S. J.; Azhar, B.; Miller, T. W.; Franco, N.; Cherney, M. M.; Lee, A. J.; Burstyn, J. N.; Fukuto, J. M.; Megson, I. L.; Ford, P. C. *J. Med. Chem.* **2010**, *53*, 715–722.

(15) (a) Ferguson, J.; Tobe, M. L. *Inorg. Chim. Acta* **1970**, *4*, 109–112. (b) Poon, C. K.; Pun, K. C. *Inorg. Chem.* **1980**, *19* (2), 568–569.

(16) Kudo, S.; Bourassa, J. L.; Boggs, S. E.; Sato, Y.; Ford, P. C. *Anal. Biochem.* **1997**, *247*, 193–202.

(17) (a) A photograph of a Schlenk cuvette is shown in the supporting information of ref .15b. (b) Rimmer, R. D.; Richter, H.; Ford, P C. *Inorg. Chem.* **2010**, *49*, 1180–1185.

(18) Calvert, J. G.; Pitts, J. N. *Photochemistry*; John Wiley & Sons: New York, 1966.

(19) Wegner, E. E.; Adamson, A. W. *J. Am. Chem. Soc.* **1966**, *88*, 394–404.

(20) Lazos, G. P.; Hoffman, B. M.; Franz, C. G. *QCPE program number 265*; Quantum Chemistry Program Exchange, Chemistry Dept., Indiana University: Bloomington,IN.

(21) *SMART Software Users Guide*, Version 5.1; Bruker Analytical X-ray Systems, Inc.: Madison, WI, 1999.

(22) *SAINT Software Users Guide*, Version 5.1; Bruker Analytical X-ray Systems, Inc.: Madison, WI, 1999.

(23) Sheldrick, G. M. *SHELXTL*, Version 6.12; Bruker Analytical X-ray Systems, Inc.: Madison, WI, 2001.

(24) Turnbull, C. M.; Marcarino, P.; Sheldrake, T. A.; Lazzarato, L.; Cena, C.; Fruttero, R.; Gasco, A.; Fox, S.; Megson, I. L.; Rossi, A. G. *J. Inflammation* **2008**, *5*, 12.

(25) Kutal, C.; Adamson, A. W. *J. Am. Chem. Soc.* **1971**, *93* (21), 5581–5582.

(26) Goldstein, S.; Czapski, G. *Free Radical Biol. Med.* **1995**, *19*, 505–10.

(27) Beckman, J. S.; Koppenol, W. H. *Am. J. Physiol.* **1996**, *271* (5, Pt. 1), C1424–C1437.

(28) (a) Halfpenny, E.; Robinson, P. L. *J. Chem. Soc.* **1952**, 928–938. (b) Yagil, G.; Anbar, M. *J. Inorg. Nucl. Chem.* **1964**, *26*, 453–60.

(29) Pryor, W. A.; Squadrito, G. L. *Am. J. Physiol.* **1995**, *268* (5, Pt. 1), L699–L722.

(30) Ford, P. C.; Wink, D. A.; Stanbury, D. M. *FEBS Lett.* **1993**, *326*, 1–3.

(31) Winterbourn, C. C.; Hampton, M. B. *Free Radical Biol. Med.* **2008**, *45*, 549–561.

(32) Vaupel, P.; Schlenger, K.; Knoop, C.; Hockel, M. *Cancer Res.* **1991**, *51*, 3316–3322.

(33) A different result was seen with dithiothreitol (DTT), which is commonly used in biological experiments as an added reductant. The spectral changes in the presence and absence of oxygen were not analogous to those seen when GSH was present and DTT did not enhance NO production in aerated media as effectively as did GSH. This is puzzling since DTT should be nearly as good a reductant as is GSH, and needs further investigation.

(34) Andreasen, L. V.; Lorkovic, I. M.; Richter-Addo, G. B.; Ford, P. C. *Nitric Oxide* **2002**, *6*, 228–235.

(35) (a) Srinivasan, K.; Kochi, J. K. *Inorg. Chem.* **1985**, *24*, 4671–9. (b) Codd, R.; Lay, P. A. *Chem. Res. Toxicol.* **2003**, *16*, 881–892. (c) Levina, A.; Zhang, L.; Lay, P. A. *J. Am. Chem. Soc.* **2010**, *132*, 8720–8731.

(36) Bakac, A.; Espenson, J. H. *J. Phys. Chem.* **1993**, *97*, 12249–12253.

(37) Fee, W. W.; Harrowfield, J. N. B. *Aust. J. Chem.* **1969**, *23*, 1049.

(38) DeRosa, F.; Bu, X.; Pohaku, K.; Ford, P. C. *Inorg. Chem.* **2005**, *44*, 4166–4174.

(39) (a) Fleischauer, P. D.; Adamson, A. W.; Sartori, G. *Prog. Inorg. Chem.* **1972**, *17*, 1–56.(b) Wagenknecht, P. S.; Ford, P. C. *Coord. Chem. Rev.* **2011**, *255*, 591−616.

(40) (a) Duchowicz, R.; Ferrer, M. L.; Acuna, A. U. *Photochem. Photobiol.* **1998**, *68*, 494–501. (b) Pravinataa, L. C.; Youa, Y.; Ludescher, R. D. *Biophys. J.* **2005**, *88* (5), 3551–3561.

(41) Kane-Maguire, N. A. P.; Crippen, W. S.; Miller, P. K. *Inorg. Chem.* **2002**, *41*, 696–698.

(42) Vagrini, M. T.; Rutledge, W. C.; Wagenknecht, P. S. *Inorg. Chem.* **2010**, *49*, 833–838.

(43) (a) Shaw, C. A.; Webb, D. J.; Rossi, A. G.; Megson, I. L., *J. Inflammation* [1476−9255], **2009**, *6*, 14. (b) Shaw, C. A.; Taylor, E. L.; Fox, S.; Megson, I. L.; Rossi, A. G. *Free Radical Biol. Med.* **2011**, *50*, 93–101. (c) Taylor, E. L.; Rossi, A. G.; Shaw, C. A.; Dal Rio, F. P.; Haslett, C.; Megson, I. L. *Br. J. Pharmacol.* **2004**, *143*, 179–185.